

**PHENOTYPIC CHARACTERIZATION OF CLINICALLY ISOLATED  
*CLOSTRIDIODES DIFFICILE* STRAIN LC5624**

An Undergraduate Research Scholars Thesis

by

AVERY YOUNG

Submitted to the Undergraduate Research Scholars program at  
Texas A&M University  
in partial fulfillment of the requirements for the designation as an

UNDERGRADUATE RESEARCH SCHOLAR

Approved by Research Advisor:

Dr. Joseph Sorg

May 2018

Major: Molecular and Cellular Biology

# TABLE OF CONTENTS

|   | Page |
|---|------|
| ABSTRACT.....                           | 1    |
| ACKNOWLEDGMENTS .....                   | 2    |
| NOMENCLATURE .....                      | 3    |
| CHAPTER                                 |      |
| I.    INTRODUCTION .....                | 4    |
| General Physiology and Metabolism ..... | 5    |
| CRISPR-Cas9 Technology .....            | 15   |
| II.   MATERIALS AND METHODS.....        | 19   |
| Growth Conditions .....                 | 19   |
| Growth Curves.....                      | 19   |
| Preparation of Spores.....              | 19   |
| Germination Assays.....                 | 20   |
| Conjugation.....                        | 21   |
| III.  RESULTS .....                     | 22   |
| Growth Curves.....                      | 22   |
| Sporulation and Germination.....        | 23   |
| Conjugation.....                        | 25   |
| IV.  CONCLUSIONS .....                  | 27   |
| Sporulation and Germination.....        | 27   |
| Conjugation.....                        | 28   |
| Discussion.....                         | 28   |
| REFERENCES .....                        | 30   |

## ABSTRACT

Characterization of Clinically Isolated *Clostridioides difficile* Strain LC5624

Avery Young  
Department of Biology  
Texas A&M University

Research Advisor: Dr. Joseph Sorg  
Department of Biology  
Texas A&M University

*Clostridioides difficile* is a Gram-positive, anaerobic, spore-forming pathogen. Due to, in part, the highly transmissible spore morphotype, *C. difficile* infections (CDI) frequently occur in cycles of recurring disease that are accompanied by progressively severe symptoms. Unfortunately, viable treatment options have not increased in proportion to morbidity, making investigations into individual strain phenotypes necessary in the pursuit of suitable therapies.

The focus of this research was to characterize a recently-identified *C. difficile* clinical isolate (LC5624). Assessments of growth curves and sporulation, germination assays, and analyses of genome editing by previously generated CRISPR-Cas9 plasmids have been compiled to form a detailed physiological profile of *C. difficile* LC5624.

Bridging a molecular understanding of laboratory physiology to clinical disease severity aids scientific research leveled at eliminating this human pathogen. Correlating phenotypes of actively circulating strains to levels of disease severity leverages a greater understanding of the pathogen in its community evolution, and increases the success of treatment techniques employed by medical professionals facing infection in patients.

## ACKNOWLEDGEMENTS

I would like to thank Dr. Larry Kociolek of the division of Pediatric Infectious Diseases at the Feinberg School of Medicine at Northwestern University. None of this work would have been possible without his sharing of *C. difficile* clinical isolate strain LC5624.

Next, I would like to thank my faculty mentor Dr. Sorg for the opportunity to work in his laboratory, as well as his overwhelming patience and support throughout the course of this research. Working under his expertise has been one of the most exciting and rewarding experiences I have had as an undergraduate here at Texas A&M University.

Thanks also go to all the graduate students working in Dr. Sorg's laboratory for their tolerance and kindness. I would especially like to acknowledge PhD candidates Ritu Shrestha and Kathleen McAllister as my role models. It was with their patient guidance and steadfast encouragement that this research was completed.

Finally, I would like to acknowledge the friends and family that gave me the confidence to pursue this undertaking. Special credit also goes to Louie for always being excited to see me, even when I smelled like the bacteria. Thank you all for your love.

## NOMENCLATURE

|                  |   |
|------------------|---|
| AAD              | Antibiotic associated diarrhea                            |
| Cas              | CRISPR-associated systems                                 |
| CDCA             | Chenodeoxycholic acid                                     |
| CDC              | Center for Disease Control and Prevention                 |
| CDI              | <i>Clostridioides difficile</i> infection(s)              |
| CLSI             | Clinical and Laboratory Standards Institute               |
| CRISPR           | Clustered regularly interspaced short palindromic repeats |
| DPA              | Dipicolinic acid  |
| EC <sub>50</sub> | Effective Concentration 50%                               |
| PaLoc            | Pathogenicity locus                                       |
| PAM              | Protospacer-adjacent motifs                               |
| PCR              | Polymerase chain reaction                                 |
| PM               | Phenotype microarrays                                     |
| PPE              | Personal Protective Equipment                             |
| PTG              | Peptidoglycan   |
| SASP             | Small acid soluble proteins                               |
| TA               | Taurocholate  |
| TcdA             | Toxin <i>Clostridioides difficile</i> A                   |
| TcdB             | Toxin <i>Clostridioides difficile</i> B                   |

# CHAPTER I

## INTRODUCTION

*Clostridioides difficile*, one of the major pathogenic clostridia, has gained notoriety as a nosocomial pathogen due to its highly infectious spore morphotype, toxin production, and antibiotic resistance. Notably, in some areas of North America, *C. difficile* infections (CDI) have surpassed methicillin resistant *Staphylococcus aureus* (MRSA) as the top nosocomial pathogen [5, 6]. *C. difficile* begins cycles of infection in the colon, and transmits between hosts, as heat-resistant spores, via fecal-oral transmission. Essential for the pathogenesis of the vegetative form are two closely-related toxins, toxins A and B (TcdA & TcdB, respectively) [7, 8]. Clinical manifestations of CDI range from asymptomatic carrier states to potentially life threatening pseudomembranous colitis and toxic megacolon [5, 8]. Typical signs and symptoms of acute CDI include watery diarrhea, anorexia, nausea, and mild cramping.

Historically, *C. difficile* has been responsible for significant morbidity and mortality in individuals who are hospitalized, >65 years old, and with recent antibiotic exposure [8]. Occurrences in the geriatric populace are disproportionately high, such that 92% of all annual CDI deaths occur within this population [5, 9]. These patients are at particularly high risk due to disruption of the normally-protective colonic microbiome brought on by broad-spectrum antibiotic treatment (often for unrelated conditions) [10-12] and diminished immune response associated with age and medical comorbidities [13, 14]. While the substantial correlation between age and risk predicts an average 2% increase in risk a year for persons over the age of 65 [5, 15], this age demographic has been expanding in recent years. Epidemiologic profiles show increasingly pathogenic strains circulating not only in hospitalized geriatric populations,

but younger populations as well. Though generally asymptomatic, newborns, born without an established gastrointestinal microbiome, are at high risk for *C. difficile* colonization. This trend is observed in children without previous exposure to antibiotics or extensive stays in healthcare facilities [16, 17]. In addition to an expanding age range deemed at high risk, *C. difficile* also threatens populations across a number of continents. Long identified as a risk in North American and European healthcare communities, recently it has established a foothold in Asia. The current uptrend in *C. difficile* prevalence in North American and European populations likely heralds a similar pattern in Asian communities over time [8].

This increasingly global health risk has made *C. difficile* the target of novel antibiotic and non-antibiotic therapies, and has driven the innovation behind many unique avenues of research. Characterization of phenotypes seen in *C. difficile* clinical isolates confers an understanding of the pathogen faced by physicians and patients in healthcare today. Insight into the current evolutionary state of this pathogen objectively aids development of therapies and serves to curtail potential increases in pathogenicity and virulence.

### **General Physiology and Metabolism**

Comprised of approximately 180 validly described species, the genus *Clostridioides* is one of the largest bacterial genera to date [18]. Within this genus, *C. difficile* is one of only a few species that is pathogenic to humans. *C. difficile* is phylogenetically divided into 6 clades based upon PCR-ribotyping, with pathogenic strains dispersed throughout each clade. Presently, approximately 300 different *C. difficile* PCR ribotypes are known to circulate among humans and animals [19]. Historically, endemic outbreaks in clinical settings consist of one prevalent ribotype, such as the ribotype 027 [17, 19]. As other strains begin to circulate clinically, it becomes imperative to characterize various ribotypes; different strains are associated with

varying degrees of pathogenicity and can present across a wide distribution of illness severity. *C. difficile* strain LC5624 was recently isolated and belongs to ribotype 106, which has recently surpassed ribotype 027 as the most frequently identified ribotype in US hospitals [19].

*C. difficile* is a Gram-positive, strictly anaerobic, rod-shaped bacterium that forms metabolically dormant spores in response to unknown cues. Genomic analyses of various *C. difficile* strains has revealed that the majority encode Type IV pilus genes [2, 20], genes associated with the production of surface-associated fimbriae [21, 22] and flagella [23]. Flagella are important for *C. difficile* pathogenesis because they have been shown to play an active role in adherence to intestinal tissue [2, 21, 22]. Moreover, as observed in other bacteria, *C. difficile* flagella have been implicated in the development of biofilms, an extracellular matrix that protects the bacterial community from environmental stresses and enables more efficient colonization [24].

*C. difficile* colonizes the gut and obtains many of the nutrients required for growth from the host's diet, mucosal secretions and/or other resident (or dietary) microbes [17, 25]. In a study done by Scaria, Chen and Useh [17], phenotype microarrays (PMs) were used to elucidate the complete nutritional profile of six endemic *C. difficile* isolates, R20291 (ribotype 027) included. Analyses comparing these nutritional and chemical phenomes showed that while simple sugars (maltotriose, maltose,  $\alpha$ -D-glucose, D-fructose, and D-mannose) are metabolically preferred by all strains, additional complex carbohydrates such as pectin and arbutin are also consumed to support high levels of growth [17]. When compared to other strains, R20291 presented with the largest metabolic capability for the 760+ nutrient sources employed in the investigation [17]. In particular, an expanded metabolic potential was revealed through a greater ability to utilize tetrathionate, taurocholate, taurine, and a wide array of peptides [17]. Recently, Collins and



colleagues [26] found that isolates of ribotype 027 and 078 are able to utilize trehalose (a food additive) at much lower concentrations than historic isolates, suggesting that there are important differences in the metabolic requirements between strains.

The expanded metabolic potential of R20291 is likely correlated to its epidemic nature. Numerous *in vitro* experiments have demonstrated that the levels of toxin production varies several fold depending upon the type of nutrient found in laboratory growth medium [27], and more recent investigations have shown there is a complex regulatory mechanism associated with this phenomenon [28, 29]. An increase in toxin production has been specifically correlated to cues of the gut, including temperature changes, existing *C. difficile* colony density, density and metabolism of the host microbiome, and any significant reduction of available nutrients [28, 30]. Furthermore, the timing of toxin gene transcription has been correlated to the depletion of nutrients in rich medium that occurs as cells enter the stationary phase of growth [30-32]. In contrast, when other nutrients (*e.g.*, glucose, proline, butanol, cysteine, biotin, and a mixture of various amino acids) are in abundance, toxin synthesis is inhibited [30].

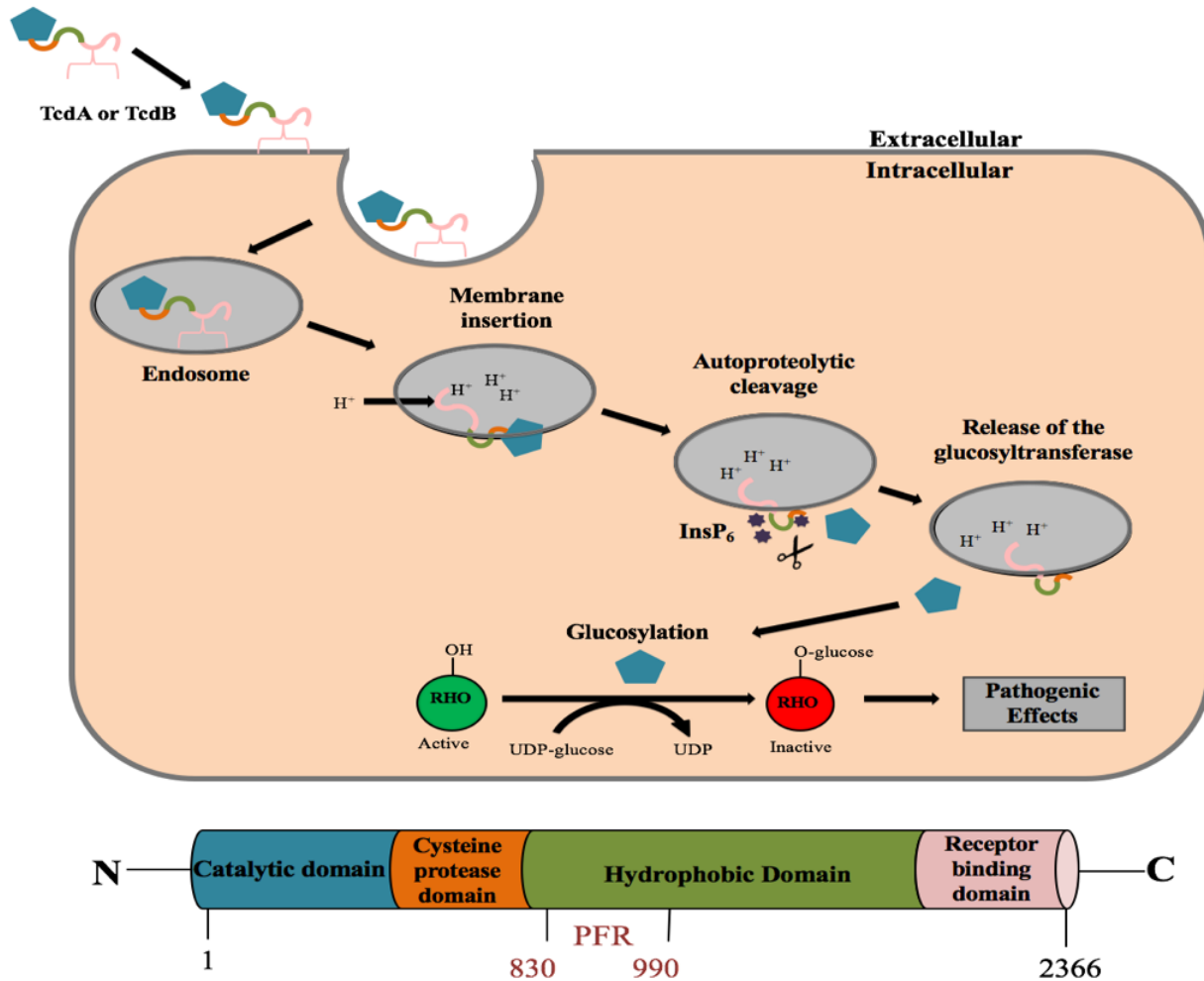


Figure 1. Cellular intoxication mechanism of TcdA and TcdB. Shown below is the domain structures of TcdB. The pore forming region (PFR) is indicated in red. Figure adapted from Awad [2].

While many aspects of the *C. difficile* infection cycle remain poorly understood, it is well established that a large proportion of disease is the synthesis of TcdA and TcdB [33-35]. Of the two toxins, TcdB is more active against tissue culture cell lines and all toxigenic strains, to date, encode *tcdB*; most, but not all encode *tcdA* [8]. As demonstrated in animal models of CDI, the absence of both of these toxins renders *C. difficile* avirulent [36].

As illustrated in **Figure 1**, the first step is receptor recognition and binding of the toxin to intestinal cells, followed by endocytosis via a clathrin- and dynamin-dependent pathway [37]. Once the toxin is endocytosed, the endosome acidifies and the toxin undergoes a conformational change. This conformational change results in the delivery domain forming a pore through which the remainder of the toxin translocates. Cytosolic exposure results in the toxin binding to the host

cell metabolite, inositol hexakisphosphate [38]. This results in autocatalytic cleavage between the cysteine protease and glucosyltransferase domains, releasing an active N-terminal glucosyltransferase into the cytosol [39].

Both TcdA and TcdB are monoglucosyltransferases that target the Rho family of small GTPases for inactivation through the covalent transfer of a glucose moiety [2]. The glycosylated GTPases are locked into an inactive conformation, which causes a number of detrimental and significant downstream events. Most critical is interference with the cell cytoskeleton. Cytoskeletal disturbance results in a loss of cellular structural integrity, marked by a decline in levels of F-actin [40], and characteristic “cell rounding” morphology that typically precedes caspase mediated cellular apoptosis [2, 41]. The pathogenic advantage of intestinal cell intoxication lies in the fact that colonic cell death disrupts the tight junctions of the intestinal epithelium [2]. This disruption undermines the host epithelia’s protective function and increases intestinal permeability. Apoptotic colonocyte death and intestinal inflammation subsequently manifests as diarrhea, the hallmark symptom of CDI [35, 42].

In order to survive outside a host in the aerobic environment, *C. difficile* cells form hardy, acid, heat and oxygen-resistant endospores through the process of sporulation. Spores are metabolically dormant infectious particles shed easily in the feces of colonized organisms and allow survival of the bacterium in an aerobic environment. As a significant agent of disease and an essential component of the *C. difficile* infection cycle, the process and mechanisms of sporulation warrant a detailed understanding.

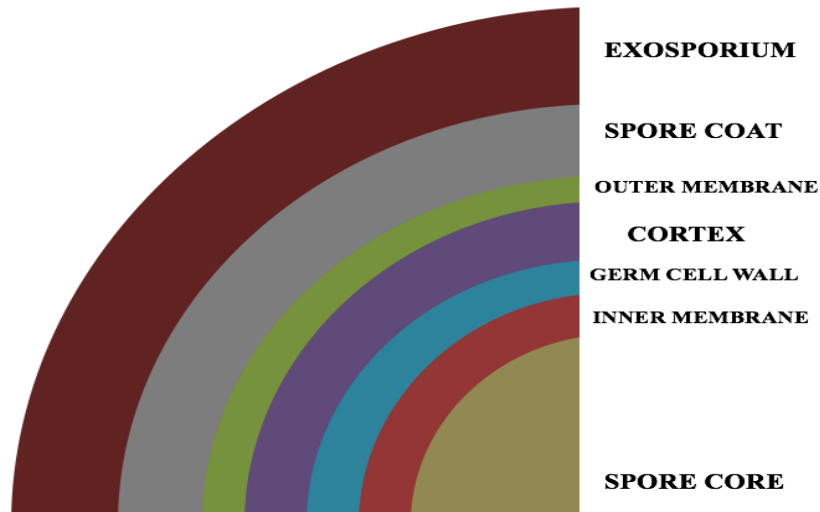


Figure 2. The main structural layers of a bacterial endospore, not drawn to scale. Sublayers present in the exosporium and spore coat are also not depicted. Figure adapted from Paredes-Sabja[1].

Endospores, widely-studied in the model organism *Bacillus subtilis*, are metabolically dormant and dehydrated structures and these features are conserved across all endospore-forming bacteria, *C. difficile* included. Each spore core contains a complete copy of the genome, as well as RNA and proteins necessary for outgrowth upon germination [1, 43, 44]. Cores are also rich in dipicolinic acid (DPA), which complexes with  $\text{Ca}^{2+}$  ions and forms a chelate that replaces water and contributes significantly to spore thermo-resistance [18, 43, 45, 46]. As shown in **Figure 2**, the core is surrounded by an inner spore membrane, a thin layer of peptidoglycan (PTG), a thick cortex PTG, an outer spore membrane, layers of coat protein, and an exosporium layer (which is present in *C. difficile* but not all endospore-forming bacteria) [43, 45, 46]. This outermost exosporium layer is the first point of contact between *C. difficile* spores and their environment, and has remarkable adherence properties [2]. The spore coat, in conjunction with the cortex and DPA, protect spores against hostile environments.

In *B. subtilis*, the model organism for studying sporulation and germination, the general sporulation process involves the formation of a swollen mother cell, and the forespore [18]. Sporulation is a tightly regulated process involving communication between the forespore and

mother cell. This communication is achieved through a cascade of alternative RNA polymerase sigma factor activation and subsequent gene expression [2, 46]. These alternative sigma factors ( $\sigma^F$ ,  $\sigma^E$ ,  $\sigma^G$  and  $\sigma^K$ ) are conserved in all endospore-forming bacteria. Interestingly, though, *C. difficile* was shown to lack the intercompartmental criss-cross communication between sigma factors present in the *B. subtilis* paradigm [1, 47-49]. Although the *C. difficile* sporulation-specific sigma factors undergo an alternate pathway of activation (**Figure 3**), Pereira [49] demonstrated that the activation of these sigma factors is compartment-specific in a manner similar to what is observed in *B. subtilis*. For example, activity of the  $\sigma^F$  and  $\sigma^G$  sigma factors is restricted to the maturing forespore and activity of  $\sigma^E$  and  $\sigma^K$  is restricted to the mother cell [1, 49].

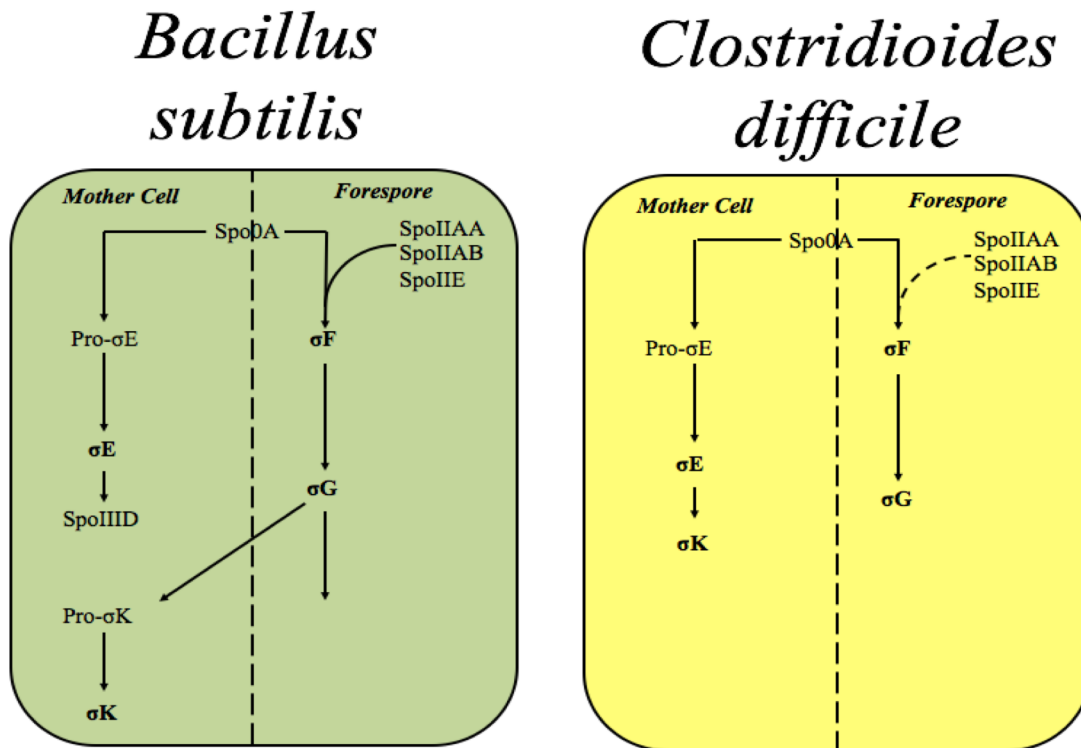


Figure 3. Models of *B. subtilis* and *C. difficile* cascading activation of four main sporulation specific sigma factors. Figure adapted from Paredes-Sabja[1].

Another notable variation from the mechanism of spore formation found in *B. subtilis*, is the fact that *C. difficile* does not use a phosphorelay in the activation of sporulation master regulator Spo0A [18]. Sporulation in *C. difficile* is alternately initiated by several orphan histidine kinases that directly phosphorylate Spo0A [50, 51]. Spo0A, conserved in all endospore forming bacteria [18, 52], is aptly named the master regulator of sporulation because genetic deletion mutants of *spo0A* result in asporogenic phenotypes [2]. As such, *spo0A* mutants are defective in host-to-host transmission [46]. It is well established that *C. difficile* sporulation frequency and yields of spore density is strain-dependent [53], however, the precise external signals necessary to initiate sporulation have yet to be definitively defined. However, it is hypothesized these signals are likely related to environmental stimuli (*e.g.*, quorum sensing or nutrient limitation) [1, 51].

High rates of CDI reoccurrence are due, in part, to ingestion of spores, which are ubiquitous in the environment of infected individuals. In animal models of CDI, *C. difficile* infected shed in excess  $10^8$  *C. difficile* spores per gram of feces [54]. Abiotic sampling confirms high levels of spore persistence in health care environments, which is unsurprising because spores demonstrate a remarkable adherence to stainless steel, a common material in hospitals [2, 55].

Spores found within the contaminated environment enter new hosts through oral ingestion. The exosporium and spore coat protect the core from the acidic environment of the stomach, which can range from pH 1.5 in humans to pH 4.3 in other mammalian hosts [56]. Under appropriate environmental conditions, spores germinate to the actively growing, toxin-producing, vegetative form. In most spore forming bacteria, *e.g.*, *B. subtilis* and *Clostridium perfringens*, germination is triggered upon activation of Ger-type receptors embedded in the

spore inner membrane by species-specific germinants [1, 46]. In contrast, *C. difficile* lacks orthologues of these classic *ger*-type germinant receptors, and instead initiates germination in response to bile acid germinants using a pseudoprotease, CspC [57]. With its partner proteins, CspB and CspA, CspC promotes the proteolytic activation of SleC, a spore cortex degrading enzyme that is packaged into spores as a zymogen [46, 57]. Activation of pro-SleC leads to degradation of cortex PTG, which coincides with release of monovalent ions ( $H^+$ ,  $Na^+$ ,  $K^+$ ) and DPA from the core [1, 18, 58, 59]. Also timed with the release of monovalent cations and cortex hydrolysis is the protease-mediated breakdown of  $\alpha$  and  $\beta$  type small acid soluble proteins (SASP) [60], which saturate the genomic DNA found in the core and contribute to spore dormancy [1, 18]. This entire process culminates in the rehydration of the core, resumption of metabolic activity, and spore outgrowth [18].

*C. difficile* germination is initiated by certain bile acids germinants and certain amino acid co-germinants [43]. As such, a large portion of spore fate in the colon depends on the secretion of specific bile acids into the duodenum by the liver and gall bladder. Bile acids are small steroid acids that aid in the absorption of fats and cholesterol [61]. There are two families of bile acids: cholic acid derivatives and chenodeoxycholic acid derivatives (CDCA) [46]. Commonly, these primary bile acids are conjugated with either a taurine (taurocholic acid, TA) or a glycine (glycocholic acid or glycochenodeoxycholic acid) [61]. The distinction between the cholic acid class and CDCA class of bile acids is significant. Sorg and Sonenshein [62 {Sorg, 2009 #102}] demonstrated that *C. difficile* spore germination is activated by cholic acid derivatives and inhibited by CDCA derivatives. In fact, most spores derived from clinical *C. difficile* isolates reach maximum germination rates only in the presence of cholic bile acid derivative TA and amino acid co-germinant glycine [63]. Cholates-containing bile salts are

usually degraded by the normal gut microflora, but upon disruption of the natural microbiome, TA concentrations persist in the colon and serve as a potent spore germinant [64]. This effect is augmented by the fact that CDCA derivatives, competitive inhibitors of TA-mediated germination, are reabsorbed by the gut more rapidly than are pro-germinatory cholic acids [2, 62]. It is also appropriate to note that historical  $EC_{50}$  values of TA are in the low millimolar range, while  $EC_{50}$  values of CDCA are in the high micromolar range.

Whilst it is understood that *C. difficile* spore germination requires additional amino acid co-germinants, the specific amino acid spore germinant receptor still remains under investigation [43]. Regardless of the receptor, glycine has proven to be the most effective amino acid co-germinant in all strains investigated thus far [65]. This is possibly due to its small, simple size, which likely promotes diffusion through spore layers, as well as the fact that glycine is utilized in metabolic Stickland reactions. Stickland reactions generate energy for some anaerobic bacteria that primarily rely on amino acids for sources of carbon and nitrogen [3]. Glycine functions as an electron acceptor during Stickland's oxidative decarboxylation and deamination of amino acids, which results in NADH and ATP [3, 30]. Additionally, glycine is easily available in host colonic environments, and can be derived from the host bile acid glycocholate through a deconjugation reaction of glycine and cholate [43, 61, 66]. Shrestha and Sorg [43], in their study of the hierarchy of amino acid co-germinants, characterized the efficiency with which various amino acid co-germinants, and their enantiomers, influenced germination. Through the calculation of  $EC_{50}$  values, derived from nontraditional enzyme kinetics since germination is a multi-enzyme process, a quantitative measure of amino acid co-germinant effectiveness was established. Based on  $EC_{50}$  data, the authors concluded that after aspartic acid, branched side chain amino acids such as valine, leucine, and isoleucine, and D-alanine, are the poorest co-germinants [43]. The precise



hierarchy of amino acid co-germinants varies by strain, but general trends suggest that a majority of both D and L-amino acids are recognized as co-germinants [64].

## CRISPR-Cas9 Technology

Contemporary strides in the field of molecular biology include the advent of CRISPR-Cas9 site directed mutagenesis. An overview mechanism of CRISPR mediated genetic exchange defense is modeled in **Figure 4**. Clustered regularly interspaced short palindromic repeats

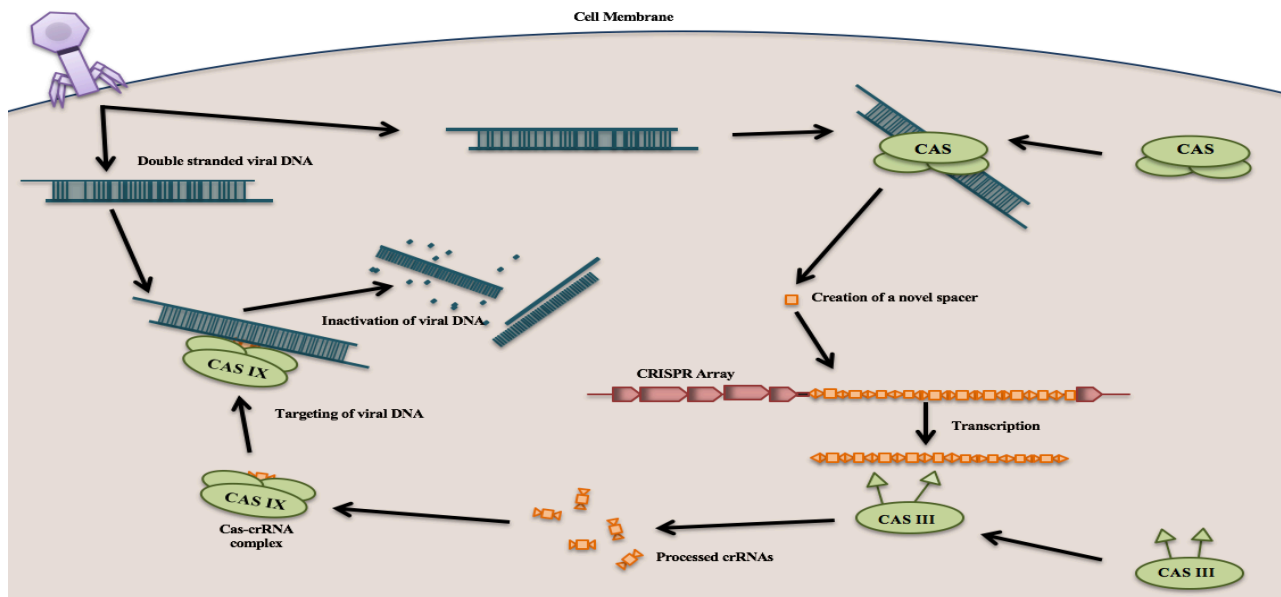


Figure 4. Overview of the CRISPR/Cas mechanism of action. After insertion of foreign DNA from phages or plasmids, a Cas complex recognizes foreign DNA and creates and inserts a novel repeat-spacer into the CRISPR array. The CRISPR repeat-spacer array is transcribed into a pre-crRNA that is processed into mature crRNA, which is used as a guide by a Cas complex to restrict the invading nucleic acid. Figure adapted from Horvath and Barrangou [4].

(CRISPR), in conjunction with CRISPR-associated (Cas) systems, function analogously to bacterial immune systems, allowing cells to adapt to foreign genetic invaders such as bacteriophages [35]. Native CRISPR systems have been shown to exist in approximately half of all sequenced bacterial genomes, *C. difficile* included [67]. The native *C. difficile* CRISPR system is likely an evolutionary response to the rich bacteriophage community of the host colon in which colonization occurs [35].

Genomic CRISPR loci, also referred to as CRISPR arrays, are organized such that conserved repeat sequences, approximately 30 bp long, are separated by similarly sized sequences called spacers [35]. Spacer sequences are variable, and are identical copies of viral or plasmid DNA encountered by the cell in a prior invasion event. These spacers are often described as past “memories” of *C. difficile* encounters, as new protospacers are sequentially added to CRISPR arrays as encounters occur. The process through which a new spacer is generated and integrated into the CRISPR loci is known as adaptation; it is this adaptive process that confers the cell with immunity from future invasions [35].

An entire CRISPR array is transcribed as single, pre-crRNA, which is then processed into smaller segments consisting of one spacer and its associated flanking repeats. These processed transcripts are referred to as CRISPR RNAs (crRNAs) [35]. Mature crRNAs associated with type 5 endonucleases effectively function as guide RNA (gRNA) [68]. Often, it is Cas9 that complexes with a gRNA, using sequence homology to induce restriction of the invading nucleic acids [3]. The extent of base pairing between the Cas complex and the targeted genetic material is critical to successful interference; in many bacterial CRISPR systems, *C. difficile* included, precise base pairing at the first position of the spacer is necessary for effective restriction [69, 70]. Another critical feature of the CRISPR defense system is its ability to discriminate between self and non-self. This identification is accomplished through the presence of protospacer-adjacent motifs (PAMs) located at either the 5' or 3' end of the invading sequence [71]. The 2-6 base pair PAM sequences are absent in CRISPR loci, thus ensuring that Cas complexes do not degrade the DNA sequence encoding the guide RNA transcripts.

*C. difficile* strain R20291 encodes nine active CRISPR arrays, and recognizes a 5'-CCW-3' PAM sequence (W denotes either an adenine or thymine base) [3, 35]. Additionally, the nine

CRISPR arrays of this strain are classified as subtype I-B [35]. Governing definitions of CRISPR-Cas subtype classifications are constructed through their specific restriction mechanisms and Cas protein composition, as well as specific PAM sequence recognition [3, 68]. A growing list of molecular biological tools has directly increased our understandings of *C. difficile* physiology and pathogenesis, but the search is never ending for more efficient techniques. Historically, TargeTron/ClosTron technology (mobile group II introns) has been most widely used in *C. difficile* genetic experimentation. However, TargeTron, and the other associated techniques (single crossover integrations of unstable plasmids, allelic-coupled exchange via *pyreE* and *codA* systems, and mariner transposition) are not without their shortcomings [3]. TargeTron technology, for example, is limited in the sense that it only creates insertion mutations, often leading to polar effects on genes downstream [3]. The advent of a CRISPR-Cas9 mutagenesis system takes advantage of the precision of the innate bacterial immune system to rapidly and efficiently introduce site specific mutations. Using this method, insertions are effectively introduced at a 20-50% rate of mutagenesis, and future development holds the potential for targeted point mutations [3].

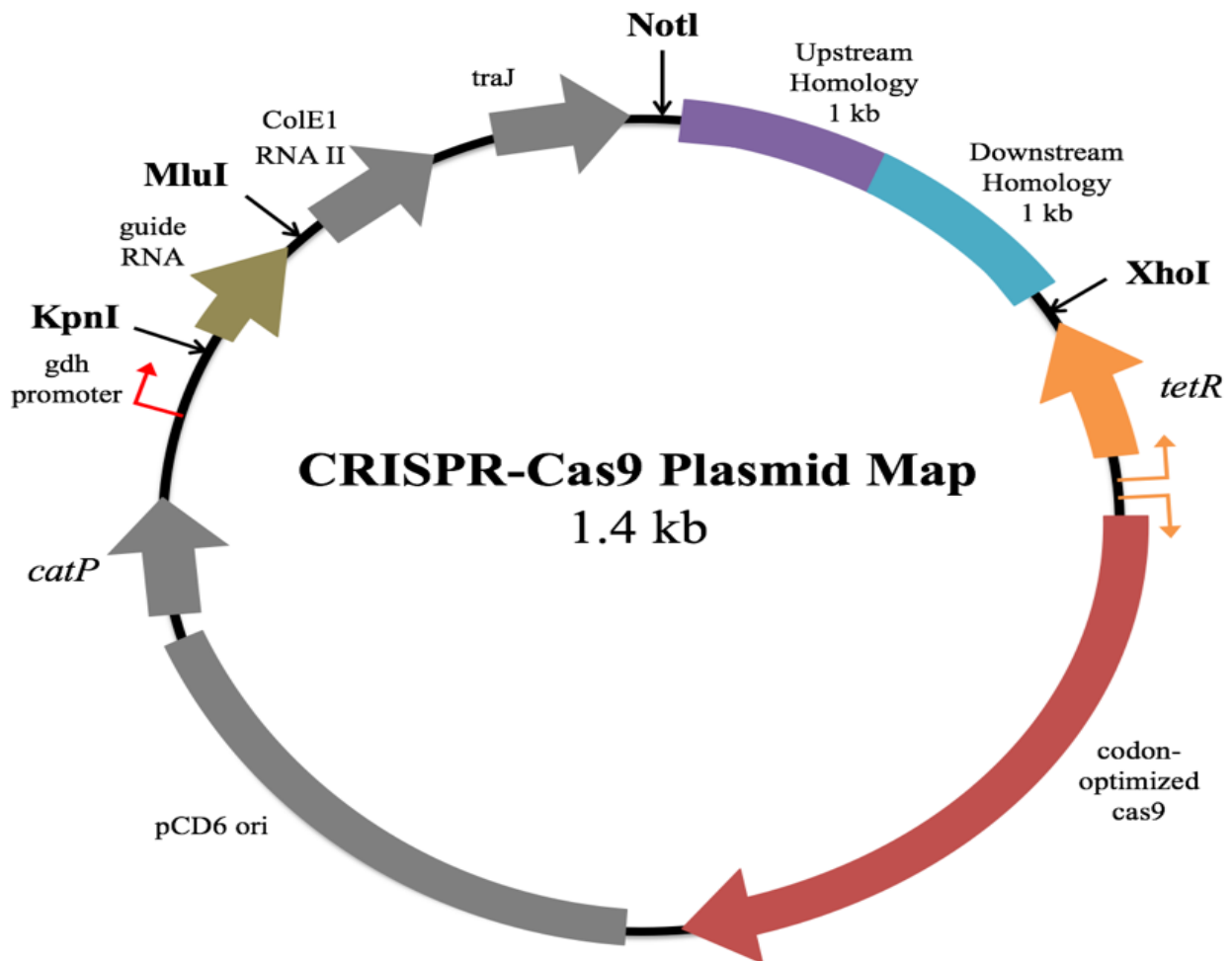


Figure 5. A model CRISPR-Cas9 plasmid map. The backbone depicted in grey consists of a *C. difficile* Gram-positive replicon origin (*oriV*, *orfB*, and *repA*), a Gram-negative replicon origin (*colE1*), and the thiamphenicol resistance marker *catP*. Depicted in color are backbone modifications and include the 1 kb upstream and downstream targeting region for homologous recombination, guide RNA under expression of *gdh* promoter, and a *tetR* promoter that regulates expression of *cas9* gene. The CRISPR plasmid utilized in experimentation was designed identically, except for *traJ* replacement with *m916* for conjugal transfer from *B. subtilis* rather than *E. coli*. Figure adapted from McAllister [3].

**Figure 5** depicts a model CRISPR-Cas9 mutagenesis plasmid. The components necessary for a functional system include a Cas9 protein, gRNA, and a region of donor DNA, which is used to create the desired mutation [3, 68, 72]. The gRNA has homology to a targeted DNA sequence and is required to induce a double stranded DNA break catalyzed by Cas9. The spliced target sequences are then vulnerable to homologous recombination that can result in both genetic deletions and insertions.

## CHAPTER II

### MATERIALS AND METHODS

#### **Growth Conditions**

*C. difficile* strains LC5624 and R20291 were routinely grown in a Model B anaerobic chamber (Coy Laboratories ) with an atmosphere of  $\geq 3\%$  H<sub>2</sub>, 5% CO<sub>2</sub>, 85% N<sub>2</sub>) at 37° C in brain heart infusion supplemented with 5 g / L yeast extract and 0.1% L-cysteine (BHIS), as described previously [46].

#### **Growth Curves**

*C. difficile* growth was monitored as previously outlined [73]. Single colonies were suspended in 5 mL liquid BHIS medium and grown overnight (~16 hours). The following day, the cultures were diluted into 20 mL of fresh BHIS media to optical density (OD) of 0.05. Growth was measure every 30 minutes for 8 hours.

#### **Preparation of Spores**

*C. difficile* spores were generated as previously described [43, 65]. *C. difficile* strains were inoculated onto BHIS agar medium. Strains were grown for 4-5 days before isolating growth by suspending in 1 mL sterile water. To promote release of the spores from the mother cells, spore suspensions were stored overnight at 4 °C. The suspensions were then washed five times (centrifuged and supernatant removed) with sterile water to remove cell debris. The spores were separated from the debris by centrifuging at  $4,000 \times g$  for 20 min in a bed of 60% sucrose. After centrifugation, the sucrose was removed, and the concentrated spores at the bottom of the tube were isolated and again washed five times with sterile water to remove the sucrose. The spores were >99% pure and heat-activated at 65 °C for 30 min before use.

Spore densities were calculated using a Petroff Hausser Counting Chamber and the manufacturer's recommend protocol [43, 74], and the final OD of the spore suspension determined.

### **Germination Assays**

The efficiencies of germination were determined as described by Shrestha *et. al.* (2018) [43, 65]. Briefly, spore germination was analyzed at 37 °C using both DPA release and optical density assays. All assays were carried out in 100  $\mu$ L total volume and performed in triplicate for each strain. As previously described, the release of DPA was monitored using a final spore density of OD = 0.5 in 50 mM HEPES buffer, pH 7.5, 250 mM NaCl, and 250  $\mu$ M of TbCl<sub>3</sub> [65]. TA and glycine were added where indicated and their concentrations varied between 0 mM and 10 mM and 0 mM and 30 mM, respectively. A 96-well plate reader at low PMT settings (excitation at 270, emission at 545 nm) was used, as described previously [75]. The optical density-based germination assay was also carried out using a plate reader at 595 nm with final 0.5 optical density spores under the conditions listed above without TbCl<sub>3</sub>.

Total DPA content of concentrated spore samples were collected according to procedures outlined briefly [75]. Spore solutions of OD = 0.5 were prepared and then 50  $\mu$ L of each sample was heated for 20 minutes in a water bath at 95 °C. Subsequently, 87.5  $\mu$ L sterile water was added to an opaque 96 well plate, along with 1  $\mu$ L of 25 mM TbCl<sub>3</sub>. 10  $\mu$ L of the boiled spore's supernatant were added to the well and read as described above. The total DPA content was run in triplicates for each strain.

To determine the effective concentration 50% values (the concentration that achieves half maximum germination rate; EC<sub>50</sub>) values for glycine, TA, and TA in the presence of the inhibitor CDCA, the kinetics of DPA release assay was monitored and the EC<sub>50</sub> determined as described

previously [43]. Briefly, spores were germinated as described above. The respective rates of germination were determined using slopes of the linear portions of germination plots. Because germination is a multi-enzyme process, data analysis resembles, but is not identical to that of single enzyme kinetics. The data was reported as the averages from independent experiments with the standard error of the mean.

### **Conjugation**

In order to determine if the LC5624 strain can be genetically modified, previously generated plasmids (empty plasmid, pJS116, and a CRISPR-Cas9 mutagenesis plasmid, pKM126) were tested for the ability to conjugate from *B. subtilis* to *C. difficile* LC5624 [3, 76]. *B. subtilis* BS49 strains were grown on Luria-Bertani (LB) medium supplemented with chloramphenicol (2.5 µg/ml), prior to matings. After overnight growth, the conjugation mixture was harvested and spread onto BHIS medium supplemented with thiamphenicol, kanamycin, and cycloserine (TKC) to counter select the *B. subtilis* donor and *C. difficile* cells that did not successfully conjugate. Thiamphenicol-positive strains of *C. difficile* were tested twice for tetracycline resistance (to screen against those transconjugants that also received a copy of the Tn916 transposon present in the *B. subtilis* donor). Thiamphenicol-positive strains that tested negative for tetracycline resistance were used. Isolated mutants were tested for the presence of the conjugated plasmid by amplifying primers for marker *catP*, as well as *tcdB* and *cas9* genes.

## CHAPTER III

### RESULTS

#### Growth Curves

**Figure 6.** Growth curve comparison of wildtype strain R20291 and clinical isolate LC5624.

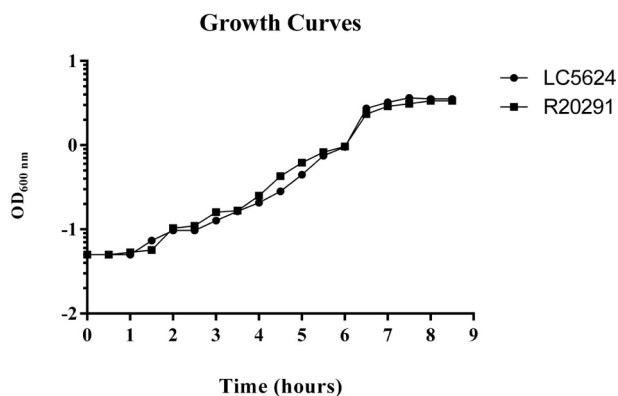


Figure 6. Growth curves of *C. difficile* LC5624 and R20291 strains in BHIS medium.

Three independent growth curves of strains R20291 and LC5624 are represented in the graph above as averages of measured OD at each half hour time interval. No significant deviation from normal logarithmic growth patterns was observed within or between strains, although clinical isolate LC5624 is capable of slightly steeper exponential growth than wildtype R20291.



## Sporulation and Germination

**Figure 7.** OD germination assays of *C. difficile* LC5624 and R20291 spores in the presence of germinants TA and glycine.

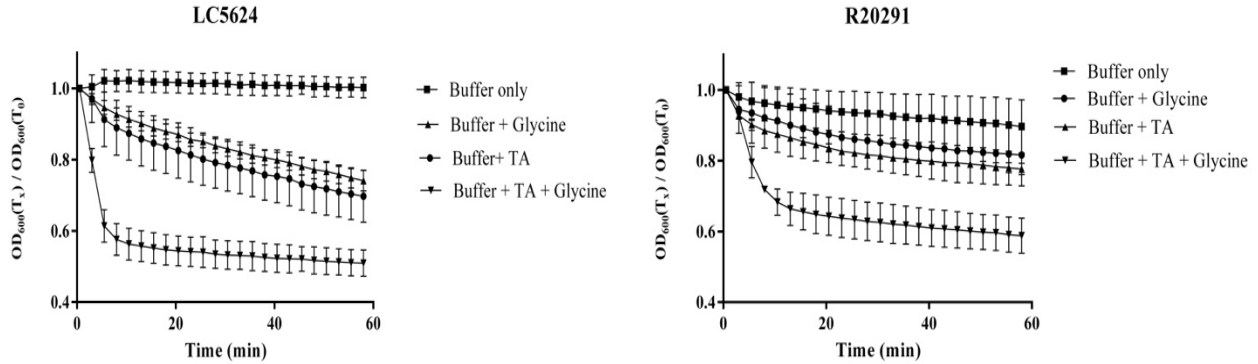


Figure 7. Germination of *C. difficile* LC5624 and R20291 spores as measured at  $OD_{600}$ . Samples were run in the presence of buffer, 100 mM TA, 100 mM glycine, and both TA and glycine.

**Figure 8.** DPA release assays of *C. difficile* LC5624 and R20291 spores in the presence of germinants TA and glycine.

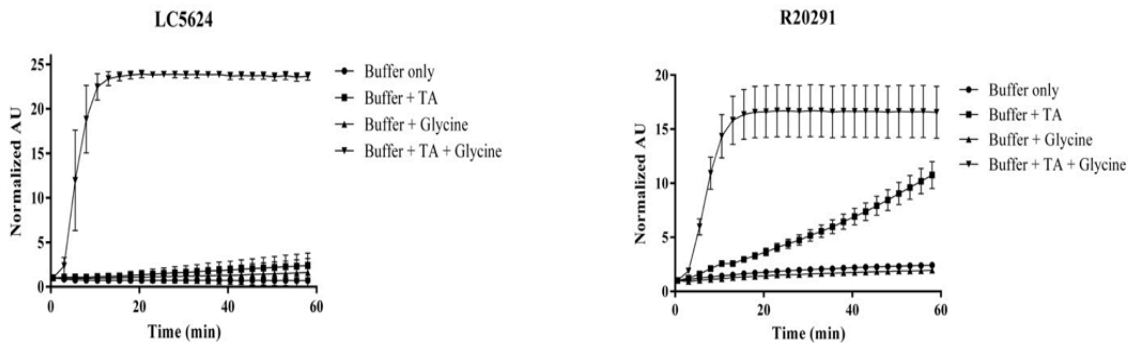


Figure 8. Germination of *C. difficile* LC5624 and R20291 spores as measured through terbium assays. Samples were run in the presence of buffer, 100 mM TA, 100 mM glycine, and both TA and glycine.

Optical density assays of *C. difficile* LC5624 and R20291 spore germination are depicted in Figure 7. DPA release assays of *C. difficile* LC5624 and R20291 are depicted in Figure 8. All OD and terbium germination assays are represented as averages of three independent trials.

During optical density assays, *C. difficile* LC5624 spores in the presence of TA and glycine showed a steeper decline in measured OD as compared to wildtype R20291 spores. As expected, spores derived from either *C. difficile* LC5624 or R20291 demonstrated minimal OD

loss in the presence of buffer alone. Notably, however, *C. difficile* LC5624 spores showed a steeper decline in measured OD than R20291 wildtype spores when in the presence of TA or glycine. This drop in OD was not correlated to an increase in fluorescence during terbium assays, as evidenced in Figure 8, suggesting that no DPA was released from the core and germination was not actually initiated.

Comparisons of the maximum fluorescence in the DPA release assays of both *C. difficile* LC5624 and R20291 (Figure 8) suggest that *C. difficile* LC5624 spores contain and release greater amounts of DPA than *C. difficile* R20291 spores. When the total DPA content present within the *C. difficile* LC5624 spores was compared to *C. difficile* R20291, *C. difficile* LC5624 contained ~50% more DPA (Figure 9). In the absence of either TA or glycine, *C. difficile* LC5624 spores show only minimal fluorescence, indicating that the spores are not germinating (Figure 8). In comparison, wildtype R20291 spores were capable of releasing DPA in the presence of TA alone. However, this did not correlate with a loss in OD. Subsequent work by a graduate student in the lab has shown that this release in DPA is due to the Tb<sup>3+</sup> ions affecting germination in an unknown way.

**Table 1.** Comparison of EC<sub>50</sub> and K<sub>i</sub> values for known germinants and inhibitors between *C. difficile* wildtype strain R20291 and clinical isolate LC5624.

|   | R20291                  | LC5624                 |
|---|-------------------------|------------------------|
| Ribotype                                  | 027                     | 106                    |
| EC <sub>50</sub> Taurocholate (mM)        | 1.20 ± 0.13             | 0.127 ± 0.02           |
| EC <sub>50</sub> Glycine (mM)             | 0.550 ± 0.10            | 0.250 ± 0.05           |
| K <sub>i</sub> Chenodeoxycholic Acid (mM) | 0.423                   | 0.268                  |
| Spore Density                             | 6.125 × 10 <sup>8</sup> | 7.01 × 10 <sup>8</sup> |

Note: EC<sub>50</sub> and K<sub>i</sub> values represent the average from three independent experiments ± the standard error of the mean. Spore densities were calculated from samples at an optical density of 0.25.

The concentrations of TA and glycine necessary to attain half maximal germination rates were quantified using DPA release assays. In these calculations, a lower EC<sub>50</sub> value indicates a

more efficient interaction with substrate and subsequently, more efficient germination. Wildtype R20291 spores require over 9 times the concentration of TA and 2.2 times the concentration of glycine than do *C. difficile* LC5624 spores to induce half maximal germination rates (Table 1). In regards to inhibition, *C. difficile* R20291 spores were inhibited at approximately 1.6 times greater concentrations of CDCA than *C. difficile* LC5624 spores (Table 1).

**Figure 9.** Total DPA content at OD 0.25.

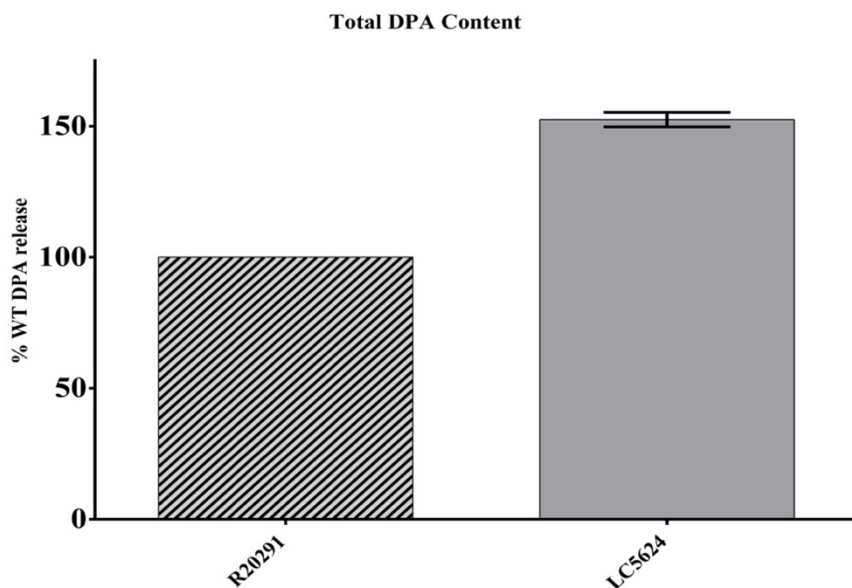


Figure 9. DPA release by *C. difficile* strains LC5624 and R20291. Total DPA content was normalized to the amount of DPA measured in *C. difficile* R20291.

Figure 9 describes the total DPA total content of R20291 and LC5624 spores respectively.

### Conjugation

CRISPR-conjugation protocol was executed multiple times using both a CRISPR plasmid (pKM126) and a control plasmid (pJS116). A total of 2 colonies yielded tetracycline-sensitive colonies of pJS116 in both *C. difficile* LC5624 and *C. difficile* R20291 strains, but no successful experiment yielded pKM126 in either strain. PCR amplification confirmed the successful

conjugation of pJS116 into both *C. difficile* LC5624 and *C. difficile* R20291. Experiments are ongoing to introduce the pKM126 CRISPR-Cas9 plasmid into these strains. But, because *C. difficile* LC5624 can take up the pJS116 plasmid, this strain may be genetically tractable.

## CHAPTER IV

### CONCLUSIONS

#### **Sporulation and Germination**

As seen in Table 1, LC5624 cultures yield a quantity of spores that is approximately 14% denser than that of wildtype R20291. These same spores, as evidenced in Figure 9, contain over 50% greater DPA content. While it is not undue to suggest that the increased density of LC5624 spores contributes to the increase seen in total DPA content, it is unlikely that 14% greater spore density returns over 50% more DPA. Instead, it is more reasonable a slight difference in sporulation between the two strains exists. It is therefore presumed that LC5624 spores are morphologically smaller, with each spore containing a greater density of DPA in its core. Furthermore, this increased capacity for DPA content in LC5624 is important in spore transmission, as it is the DPA-chelate of the core that maintains the endospore in a desiccated state until the time of germination. Greater concentrations of the core's DPA-chelate confer LC5624 spores a competitive edge in endospore resistance and subsequently, transmission.

Arguably the most notable dimension of the LC5624 germination profile is the fact that LC5624 shows a significantly heightened sensitivity to both bile acid germinants and inhibitors. Based on calculated  $EC_{50}$  values, LC5624 spores are more sensitive to the bile acid germinant taurocholate and amino acid co-germinant glycine than are R20291 spores. Similarly, based on calculated  $K_i$  values, LC5624 spores are more sensitive the bile acid inhibitor chenodeoxycholic acid than are R20291 spores. This aspect of the germination profile may be misleading if not viewed in context of a typical transmission cycle. Inside a host colon, the typical endospore will be exposed to TA, glycine and CDCA. For R20291, the  $K_i$  of the CDCA inhibitor is less than

that of the EC<sub>50</sub> of both primary germinant TA and co-germinant glycine. This means lesser concentrations of CDCA are required to inhibit germination in R20291, and greater concentrations of TA and glycine are necessary to initiate germination. LC5624, in contrast, sees EC<sub>50</sub> values for primary germinant TA and co-germinant glycine that are less than that of the inhibitory CDCA K<sub>i</sub> value. This means that lesser concentrations of TA and glycine are necessary to initiate germination and greater concentrations of CDCA are required to inhibit germination. Such variance in spore germination sensitivities carries impactful consequences in regards to infection; a spore from strain LC5624 is much more likely to germinate in the presence of typical concentrations of bile acids than is a spore of R20291.

### **Conjugation**

Conjugation experiments were successful in generating *C. difficile* colonies carrying an integrated pJS116 control plasmid for both strains. This demonstrates that both strains are capable of receiving DNA by conjugation and suggests that the LC5624 strain may be open to genetic manipulation by molecular biologists using CRISPR-Cas9 systems. A strong case remains for the potential of future success in this experimental capacity; it will certainly be pursued in future undertakings.

### **Discussion**

Wildtype strain R20291 was cultured during an epidemic outbreak of CDI in the early 2000's; clinical isolate LC5624 was cultured in 2017. As evidenced in the germination profile of *C. difficile* isolate LC5624, only little more than a decade was necessary for this specific strain of *C. difficile* to adapt increasingly deviant characteristics. While it is not suitable to suggest this uptrend in virulence is omnipresent in all actively circulating strains of ribotype 106, there is no

evidence to indicate such an increase in hypervirulence would not be modeled in other strains. Further investigations into other strains would certainly prove appropriate in this regard.

The uptrend in virulence seen in *C. difficile* isolate LC5624 is why the continuous correlation of clinical isolates, their unique phenotypes, and levels of disease severity is vital to understating the pathology of this human pathogen. In order to objectively aid both the development of therapies and curtail increases in pathogenicity and virulence, continued snapshots of the pathogen in its evolution are necessary.

## REFERENCES

1. Paredes-Sabja, D., A. Shen, and J.A. Sorg, *Clostridium difficile* spore biology: sporulation, germination, and spore structural proteins. Trends Microbiol, 2014. **22**(7): p. 406-16.
2. Awad, M.M., et al., *Clostridium difficile* virulence factors: Insights into an anaerobic spore-forming pathogen. Gut Microbes, 2014. **5**(5): p. 579-93.
3. McAllister, K.N., et al., *Using CRISPR-Cas9-mediated genome editing to generate C. difficile mutants defective in selenoproteins synthesis*. Sci Rep, 2017. **7**(1): p. 14672.
4. Horvath, P. and R. Barrangou, *CRISPR/Cas, the immune system of bacteria and archaea*. Science, 2010. **327**(5962): p. 167-70.
5. Keller, J.M. and C.M. Surawicz, *Clostridium difficile* infection in the elderly. Clin Geriatr Med, 2014. **30**(1): p. 79-93.
6. Miller, B.A., et al., *Comparison of the burdens of hospital-onset, healthcare facility-associated Clostridium difficile Infection and of healthcare-associated infection due to methicillin-resistant Staphylococcus aureus in community hospitals*. Infect Control Hosp Epidemiol, 2011. **32**(4): p. 387-90.
7. Kelly, C.P. and J.T. LaMont, *Clostridium difficile--more difficult than ever*. N Engl J Med, 2008. **359**(18): p. 1932-40.
8. Burke, K.E. and J.T. Lamont, *Clostridium difficile* infection: a worldwide disease. Gut Liver, 2014. **8**(1): p. 1-6.
9. Rineh, A., et al., *Clostridium difficile* infection: molecular pathogenesis and novel therapeutics. Expert Rev Anti Infect Ther, 2014. **12**(1): p. 131-50.
10. Edlund, C. and C.E. Nord, *Effect of quinolones on intestinal ecology*. Drugs, 1999. **58** Suppl 2: p. 65-70.



11. Johnson, S., *Recurrent Clostridium difficile infection: a review of risk factors, treatments, and outcomes*. J Infect, 2009. **58**(6): p. 403-10.
12. Pepin, J., et al., *Emergence of fluoroquinolones as the predominant risk factor for Clostridium difficile-associated diarrhea: a cohort study during an epidemic in Quebec*. Clin Infect Dis, 2005. **41**(9): p. 1254-60.
13. Kyne, L., et al., *Asymptomatic carriage of Clostridium difficile and serum levels of IgG antibody against toxin A*. N Engl J Med, 2000. **342**(6): p. 390-7.
14. Kyne, L., et al., *Association between antibody response to toxin A and protection against recurrent Clostridium difficile diarrhoea*. Lancet, 2001. **357**(9251): p. 189-93.
15. McDonald, L.C., M. Owings, and D.B. Jernigan, *Clostridium difficile infection in patients discharged from US short-stay hospitals, 1996-2003*. Emerg Infect Dis, 2006. **12**(3): p. 409-15.
16. Tschudin-Sutter, S., et al., *Distinguishing community-associated from hospital-associated Clostridium difficile infections in children: implications for public health surveillance*. Clin Infect Dis, 2013. **57**(12): p. 1665-72.
17. Scaria, J., et al., *Comparative nutritional and chemical phenome of Clostridium difficile isolates determined using phenotype microarrays*. Int J Infect Dis, 2014. **27**: p. 20-5.
18. Durre, P., *Physiology and Sporulation in Clostridium*. Microbiol Spectr, 2014. **2**(4): p. TBS-0010-2012.
19. Janezic, S. and M. Rupnik, *Genomic diversity of Clostridium difficile strains*. Res Microbiol, 2015. **166**(4): p. 353-60.
20. Melville, S. and L. Craig, *Type IV pili in Gram-positive bacteria*. Microbiol Mol Biol Rev, 2013. **77**(3): p. 323-41.
21. Borriello, S.P., et al., *Mucosal association by Clostridium difficile in the hamster gastrointestinal tract*. J Med Microbiol, 1988. **25**(3): p. 191-6.

22. Taha, S., et al., *Toxin production by and adhesive properties of Clostridium difficile isolated from humans and horses with antibiotic-associated diarrhea*. *Comp Immunol Microbiol Infect Dis*, 2007. **30**(3): p. 163-74.
23. Pituch, H., et al., *Variable flagella expression among clonal toxin A-/B+ Clostridium difficile strains with highly homogeneous flagellin genes*. *Clin Microbiol Infect*, 2002. **8**(3): p. 187-8.
24. Ethapa, T., et al., *Multiple factors modulate biofilm formation by the anaerobic pathogen Clostridium difficile*. *J Bacteriol*, 2013. **195**(3): p. 545-55.
25. Fischbach, M.A. and J.L. Sonnenburg, *Eating for two: how metabolism establishes interspecies interactions in the gut*. *Cell Host Microbe*, 2011. **10**(4): p. 336-47.
26. Collins, J., et al., *Dietary trehalose enhances virulence of epidemic Clostridium difficile*. *Nature*, 2018. **553**(7688): p. 291-294.
27. Mahe, S., G. Corthier, and F. Dubos, *Effect of various diets on toxin production by two strains of Clostridium difficile in gnotobiotic mice*. *Infect Immun*, 1987. **55**(8): p. 1801-5.
28. Hryckowian, A.J., K.M. Pruss, and J.L. Sonnenburg, *The emerging metabolic view of Clostridium difficile pathogenesis*. *Curr Opin Microbiol*, 2017. **35**: p. 42-47.
29. Bouillaut, L., et al., *Effects of surotomycin on Clostridium difficile viability and toxin production in vitro*. *Antimicrob Agents Chemother*, 2015. **59**(7): p. 4199-205.
30. Bouillaut, L., et al., *Integration of metabolism and virulence in Clostridium difficile*. *Res Microbiol*, 2015. **166**(4): p. 375-83.
31. Dupuy, B. and A.L. Sonenshein, *Regulated transcription of Clostridium difficile toxin genes*. *Mol Microbiol*, 1998. **27**(1): p. 107-20.
32. Hundesberger, T., et al., *Transcription analysis of the genes tcdA-E of the pathogenicity locus of Clostridium difficile*. *Eur J Biochem*, 1997. **244**(3): p. 735-42.

33. Deneve, C., et al., *Effects of subinhibitory concentrations of antibiotics on colonization factor expression by moxifloxacin-susceptible and moxifloxacin-resistant Clostridium difficile strains*. Antimicrob Agents Chemother, 2009. **53**(12): p. 5155-62.
34. Dupuy, B., et al., *Clostridium difficile toxin synthesis is negatively regulated by TcdC*. J Med Microbiol, 2008. **57**(Pt 6): p. 685-9.
35. Boudry, P., et al., *Function of the CRISPR-Cas System of the Human Pathogen Clostridium difficile*. MBio, 2015. **6**(5): p. e01112-15.
36. Geric, B., et al., *Binary toxin-producing, large clostridial toxin-negative Clostridium difficile strains are enterotoxic but do not cause disease in hamsters*. J Infect Dis, 2006. **193**(8): p. 1143-50.
37. Papatheodorou, P., et al., *Clostridial glucosylating toxins enter cells via clathrin-mediated endocytosis*. PLoS One, 2010. **5**(5): p. e10673.
38. Egerer, M., et al., *Autocatalytic processing of Clostridium difficile toxin B. Binding of inositol hexakisphosphate*. J Biol Chem, 2009. **284**(6): p. 3389-95.
39. Pruitt, R.N., et al., *Structure-function analysis of inositol hexakisphosphate-induced autoprocessing in Clostridium difficile toxin A*. J Biol Chem, 2009. **284**(33): p. 21934-40.
40. Carter, G.P., J.I. Rood, and D. Lyras, *The role of toxin A and toxin B in the virulence of Clostridium difficile*. Trends Microbiol, 2012. **20**(1): p. 21-9.
41. Gerhard, R., et al., *Glucosylation of Rho GTPases by Clostridium difficile toxin A triggers apoptosis in intestinal epithelial cells*. J Med Microbiol, 2008. **57**(Pt 6): p. 765-70.
42. Just, I., et al., *Glucosylation of Rho proteins by Clostridium difficile toxin B*. Nature, 1995. **375**(6531): p. 500-3.
43. Shrestha, R. and J.A. Sorg, *Hierarchical recognition of amino acid co-germinants during Clostridioides difficile spore germination*. Anaerobe, 2017. **49**: p. 41-47.

44. Bhattacharjee, D., K.N. McAllister, and J.A. Sorg, *Germinants and Their Receptors in Clostridia*. J Bacteriol, 2016. **198**(20): p. 2767-75.
45. Setlow, P., *Spore Resistance Properties*. Microbiol Spectr, 2014. **2**(5).
46. Bhattacharjee, D., et al., *Reexamining the Germination Phenotypes of Several Clostridium difficile Strains Suggests Another Role for the CspC Germinant Receptor*. J Bacteriol, 2015. **198**(5): p. 777-86.
47. de Hoon, M.J., P. Eichenberger, and D. Vitkup, *Hierarchical evolution of the bacterial sporulation network*. Curr Biol, 2010. **20**(17): p. R735-45.
48. Fimlaid, K.A., et al., *Global analysis of the sporulation pathway of Clostridium difficile*. PLoS Genet, 2013. **9**(8): p. e1003660.
49. Pereira, F.C., et al., *The spore differentiation pathway in the enteric pathogen Clostridium difficile*. PLoS Genet, 2013. **9**(10): p. e1003782.
50. Steiner, E., et al., *Multiple orphan histidine kinases interact directly with Spo0A to control the initiation of endospore formation in Clostridium acetobutylicum*. Mol Microbiol, 2011. **80**(3): p. 641-54.
51. Higgins, D. and J. Dworkin, *Recent progress in Bacillus subtilis sporulation*. FEMS Microbiol Rev, 2012. **36**(1): p. 131-48.
52. Brown, D.P., et al., *Characterization of spo0A homologues in diverse Bacillus and Clostridium species identifies a probable DNA-binding domain*. Mol Microbiol, 1994. **14**(3): p. 411-26.
53. Burns, D.A. and N.P. Minton, *Sporulation studies in Clostridium difficile*. J Microbiol Methods, 2011. **87**(2): p. 133-8.
54. Lawley, T.D., et al., *Antibiotic treatment of clostridium difficile carrier mice triggers a supershedder state, spore-mediated transmission, and severe disease in immunocompromised hosts*. Infect Immun, 2009. **77**(9): p. 3661-9.

55. Joshi, L.T., et al., *Contribution of spores to the ability of Clostridium difficile to adhere to surfaces*. Appl Environ Microbiol, 2012. **78**(21): p. 7671-9.
56. Beasley, D.E., et al., *The Evolution of Stomach Acidity and Its Relevance to the Human Microbiome*. PLoS One, 2015. **10**(7): p. e0134116.
57. Francis, M.B., et al., *Bile acid recognition by the Clostridium difficile germinant receptor, CspC, is important for establishing infection*. PLoS Pathog, 2013. **9**(5): p. e1003356.
58. Sebahia, M., et al., *The multidrug-resistant human pathogen Clostridium difficile has a highly mobile, mosaic genome*. Nat Genet, 2006. **38**(7): p. 779-86.
59. Paredes-Sabja, D., P. Setlow, and M.R. Sarker, *Germination of spores of Bacillales and Clostridiales species: mechanisms and proteins involved*. Trends Microbiol, 2011. **19**(2): p. 85-94.
60. Setlow, P., *I will survive: DNA protection in bacterial spores*. Trends Microbiol, 2007. **15**(4): p. 172-80.
61. Ridlon, J.M., D.J. Kang, and P.B. Hylemon, *Bile salt biotransformations by human intestinal bacteria*. J Lipid Res, 2006. **47**(2): p. 241-59.
62. Sorg, J.A. and A.L. Sonenshein, *Inhibiting the initiation of Clostridium difficile spore germination using analogs of chenodeoxycholic acid, a bile acid*. J Bacteriol, 2010. **192**(19): p. 4983-90.
63. Sorg, J.A. and A.L. Sonenshein, *Bile salts and glycine as cogermnants for Clostridium difficile spores*. J Bacteriol, 2008. **190**(7): p. 2505-12.
64. Howerton, A., N. Ramirez, and E. Abel-Santos, *Mapping interactions between germinants and Clostridium difficile spores*. J Bacteriol, 2011. **193**(1): p. 274-82.
65. Shrestha, R., S.W. Lockless, and J.A. Sorg, *A Clostridium difficile alanine racemase affects spore germination and accommodates serine as a substrate*. J Biol Chem, 2017. **292**(25): p. 10735-10742.

66. Ridlon, J.M., et al., *Bile acids and the gut microbiome*. *Curr Opin Gastroenterol*, 2014. **30**(3): p. 332-8.
67. Grissa, I., G. Vergnaud, and C. Pourcel, *The CRISPRdb database and tools to display CRISPRs and to generate dictionaries of spacers and repeats*. *BMC Bioinformatics*, 2007. **8**: p. 172.
68. Doudna, J.A. and E. Charpentier, *Genome editing. The new frontier of genome engineering with CRISPR-Cas9*. *Science*, 2014. **346**(6213): p. 1258096.
69. Stoll, B., et al., *Requirements for a successful defence reaction by the CRISPR-Cas subtype I-B system*. *Biochem Soc Trans*, 2013. **41**(6): p. 1444-8.
70. Semenova, E., et al., *Interference by clustered regularly interspaced short palindromic repeat (CRISPR) RNA is governed by a seed sequence*. *Proc Natl Acad Sci U S A*, 2011. **108**(25): p. 10098-103.
71. Sorek, R., C.M. Lawrence, and B. Wiedenheft, *CRISPR-mediated adaptive immune systems in bacteria and archaea*. *Annu Rev Biochem*, 2013. **82**: p. 237-66.
72. Sternberg, S.H. and J.A. Doudna, *Expanding the Biologist's Toolkit with CRISPR-Cas9*. *Mol Cell*, 2015. **58**(4): p. 568-74.
73. Stephen, A.S., et al., *In vitro growth characteristics and volatile sulfur compound production of Solobacterium moorei*. *Anaerobe*, 2014. **26**: p. 53-7.
74. Treuer, R. and S.E. Haydel, *Acid-fast staining and Petroff-Hausser chamber counting of mycobacterial cells in liquid suspension*. *Curr Protoc Microbiol*, 2011. **Chapter 10**: p. Unit 10A 6.
75. Francis, M.B. and J.A. Sorg, *Dipicolinic Acid Release by Germinating Clostridium difficile Spores Occurs through a Mechanosensing Mechanism*. *mSphere*, 2016. **1**(6).
76. Bouillaut, L., S.M. McBride, and J.A. Sorg, *Genetic manipulation of Clostridium difficile*. *Curr Protoc Microbiol*, 2011. **Chapter 9**: p. Unit 9A 2.